Applied Mathematical Modelling 39 (2015) 548–558

Contents lists available at ScienceDirect

Applied Mathematical Modelling

journal homepage: www.elsevier.com/locate/apm

Tribo-dynamic model of slipper bearings

Shuo Lin, Jibin Hu *

Science and Technology on Vehicular Transmission Laboratory, Beijing Institute of Technology, Beijing, PR China

ARTICLE INFO

Article history:
Received 29 July 2013
Received in revised form 15 June 2014
Accepted 18 June 2014
Available online 24 June 2014

Keywords:
Axial pump
Film thickness measurement
Genetic algorithm
Slipper bearing
Tribo-dynamic model

ABSTRACT

In this study, we propose a tribo-dynamic model of slipper bearings in axial piston pumps and motors. We construct a unified model that considers the interaction between tribological behavior and dynamic performance. A niche genetic algorithm method is used to solve the model. The effects of cylinder speed, loading pressure, and oil viscosity on the behavior of the slipper are outlined. A test bench is established for the measurement of the slipper film thickness. We demonstrate that the elastic deformation, wearing profile, and hydrodynamic effect should be considered in the model. A high loading pressure and low speed with low viscosity will result in a low film thickness and severe tilting.

1. Introduction

Slipper bearings are essential design elements in axial piston pumps and motors, especially to meet the demand for higher efficiency and higher power density [1]. The tribological behavior of the slipper–swashplate interface is complex. Numerous motions and forces have a combined impact on the slippers. Both the tribological and dynamic behaviors have important effects on the lubrication characteristics.

This study focuses on the effects of the operating conditions on the lubrication behaviors of slipper bearings. Much research has been conducted in this field, where studies have typically focused on either the dynamic model or the tribological model, whereas the other model was evaluated using mathematical coefficients or equations. Koc [2–4] analyzed the effects of the orifice size, offset, and overclamp ratio on the lubrication of slipper bearings based on experimental research, where the measurement of the oil film thickness was discontinuous. Yamaguchi [5,6] presented a compliant model of the motions and forces on the slipper, which was analyzed experimentally and theoretically. Hooke and Li [7,8] concluded that the profile at the bottom is an important factor in hydrodynamic bearing based on an analysis of three types of profiles. Experimental results were obtained with different centrifugal loads using the same operating conditions. Ivantysynova [9,10] built a slipper-swash plate model that considered the wear of the slipper and the swash plate. The model could calculate the solid body pressure deformation, which was fixed in this case. Canbulut [11,12] used artificial neural networks to analyze the performance of slipper bearings, which included experimental results and a consideration of the elastohydrostatic problem. Manring [13] experimentally investigated the performance of slippers using different assumed socket geometries at low speed. The results showed that the leakage and capacity were affected by elastic deformation. Nie [14] built a wearing test system for hydrostatic slipper bearings to investigate the frictional properties of various materials. The reaction forces of the bearing in a water hydraulic axial piston motor were investigated without measuring the film thickness.

* Corresponding author. Tel.: +86 01068914786; fax: +86 01068914487.
E-mail address: hujibin@bit.edu.cn (J. Hu).

http://dx.doi.org/10.1016/j.apm.2014.06.009
0307-904X/

List of symbols

A_s	area of the slipper bottom (mm^2)
d_p	diameter of the piston chamber (mm)
F_d	shared friction force of the oil film (N)
F_N	oil pressure force of piston chamber (N)
F_{fit}	fitness of the individual (–)
h_p	wear height on the point B of slipper (μm)
h_m	elastic deformation (μm)
h	oil film thickness (μm)
h_o	central film thickness (μm)
$h_{\min}$	minimum film thickness (μm)
l_h	distance between the slipper bottom and the ball center (mm)
l_g	length between the slipper center of mass and the ball center (mm)
M_f	moment of the oil film (N m)
M_q	simplified overturning moment (N m)
M_d	shared friction moment of the oil film (N m)
m_s	mass of the slipper (kg)
N	size of the population (–)
n	rotation speed of cylinder ($r\ min^{-1}$)
p	pressure at an arbitrary point (Pa)
p_p	piston chamber pressure (Pa)
p_s	pocket pressure (Pa)
P_i	position of sorting (–)
Q_{in}	inlet flow rate ($L\ min^{-1}$)
Q_{out}	outlet flow rate ($L\ min^{-1}$)
R_{cp}	radius of the pitch circle (mm)
r	radius of the point B of slipper (mm)
R_i	inner radius of the sealing belt (mm)
R_e	outer radius of the sealing belt (mm)
W_{fz}	carrying force of oil film (N)
z	pressure-viscosity index
α	tilting angle (°)
β	angle of the swash plate (°)
ϕ	directional angle of point B on the slipper (°)
φ	directional angle of the slipper on the swash plate (°)
η	viscosity of oil (Pa s)
η_0	viscosity at ambient pressure
θ	directional angle of point B on the slipper (°)
ω_s	angular rate of the spin ($rad\ s^{-1}$)
ω	angular rate of cylinder ($rad\ s^{-1}$)

Bergada [15] investigated the hydrodynamic behavior of a slipper with grooves. Analytical, experimental, and CFD methods were used in their study. The niche genetic algorithm (NGA) method was introduced for the calculation of slipper lubrication performance by Liu [16]. The slipper characteristics in a steady state condition were reported.

A unified tribo-dynamic model that considers the interaction between tribological behavior and dynamical performance is introduced in a simulation of slipper bearings in the present study. The tribo-dynamic model has been used most frequently in studies of multi-body dynamics [17–20]. Recently, this model was introduced into a simulation of gear pairs. De la Cruz [21] built a tribo-dynamic model of gears as a part of a full model to study mixed thermo-elasto hydrodynamic lubrication in multi-speed transmissions. The essence and the universality of the model were not expounded in detail. De la Cruz [22] also used a transient tribo-dynamic model that considered the thermo-elastic effect in their study of compliant piston skirts.

In the present study, a tribo-dynamic model is produced that considers the fluid–solid coupling to accurately describe the behavior of slippers. The behavior of the slipper is affected by factors such as the pressure field, slipper profile, the nonuniform gap between the slipper and the swash plate, external forces and motions, and elastic deformation. These factors can be divided into tribological and dynamical components, b many parameters participate in the interactive computation between these two parts. The model is solved using the NGA method. A test bench is built for the slipper oil film. The effects of

cylinder speed, loading pressure, and the viscosity of oil on the slipper are studied. The characteristics of the oil film are evaluated, such as the central thickness, minimum film thickness, tilting angle, and pressure field. The tribo-dynamic approach used in this study is based on previous research, but the novel aspect of our study is the integration of NGA optimization.

2. Theory

In the tribo-dynamic model shown in Fig. 1, the slipper profile influences the pressure field, which is also affected by the squeezing effect of the slipper. The pressure distribution results in a change in the gap between the slipper and the swash plate. The external forces and motions provide boundary conditions for calculating the pressure and they produce hydraulic forces on the outside of the slipper. Both the contact forces coming from the slipper bearing and the elastic deformation of the slipper affect the film shape. The wearing profile caused by the tilting contact also changes the film thickness. A coupled simulation that includes these interaction effects is needed for the model.

2.1. Tribological submodel

The slipper is supported by the fluid film in the nonuniform gap between the slipper bottom and the swash plate. The film pressure is generated by the pocket pressure and the hydrodynamic effect. A cylindrical coordinate system is used in the tribological submodel, which is based on the Reynolds equation.

Fig. 2 shows the tilting state description of the slipper oil film. When the slipper is tilted, the oil film at arbitrary point B (r,θ) can be described by the tilting angle α, the directional angle ϕ, and the central film thickness h_o:

$$h = h_o + \alpha r\cos(\theta - \phi) + h_p + h_m, \quad R_i \leqslant r \leqslant R_e, \tag{1}$$

where h_p is the wear height on point B of the slipper. The wearing profile data were determined experimentally and the arc shape of the sealing belt was described by fitting an equation. h_m is the elastic deformation obtained by a finite element modeling method, which changes over time in the simulation.

The squeezing effect can be ignored when the slipper is always under high loading pressure and the change in the extra load is slight. The analysis is carried out isothermally. The pressure governing equation is as follows:

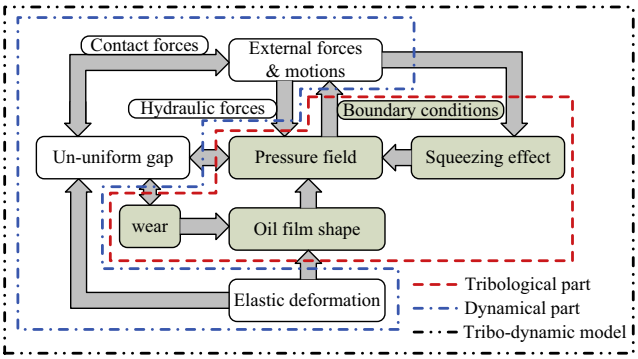

Fig. 1. Tribo-dynamic model of slipper bearings.

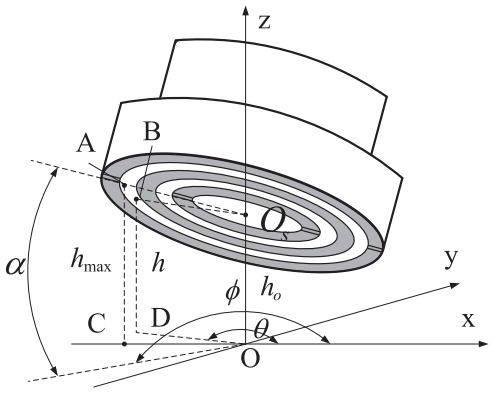

Fig. 2. Tilting state description of the slipper oil film.

$$\frac{\partial}{r\partial r}\left(rh^3\frac{\partial p}{\partial r}\right)+\frac{1}{r^2}\frac{\partial}{\partial\theta}\left(h^3\frac{\partial p}{\partial\theta}\right)=6\eta\left[\omega R\cos\theta\frac{\partial h}{\partial r}-\left(\omega+\omega_s+\frac{\omega R\sin\theta}{r}\right)\frac{\partial h}{\partial\theta}\right], \tag{2}$$

where p is the pressure at an arbitrary point, η is the viscosity of oil, ω_s is the angular rate of the spin, ω is the angular rate of the cylinder, and R is the radius of the pitch circle.

The Reynolds pressure boundary condition is used in the present analysis. The oil film pressure is equal to the atmospheric pressure in the cavitation:

$$p(\theta,R_i)=p_s;\quad p(\theta,R_e)=0, \tag{3}$$

where p_s is the pocket pressure. The geometric characteristics of the sealing belt affect the pressure periodically, thus the periodic pressure boundary condition is as follows.

$$p(0,r)=p(2\pi,r). \tag{4}$$

For isothermal conditions, Roelands' equation reduces to:

$$\eta=\eta_0\exp\left\{(\ln\eta_0+9.67)\left[\left(1+5.1\times10^{-9}p\right)^z-1\right]\right\}, \tag{5}$$

where η_0 is the viscosity at ambient pressure and z is the pressure-viscosity index. The index of z ranges from approximately 0.1–1.5 for various lubricants.

2.2. Simplified dynamical submodel

The pressure field of the slipper film is related to the forces/torques and motions. The slipper can be simplified as a thrust bearing, which slides on the swash plate at high speed. Several forces act on the slipper, including the impacting force F_N from the oil pressure of the piston chamber,

$$F_N=\frac{\pi d_p^2 p_p}{4\cos\beta}, \tag{6}$$

the carrying force W_{fz},

$$W_{fz}=\sum_{i,j}p_{ij}r_j\Delta r\Delta\theta+\pi p_s A_s, \tag{7}$$

the torque of the oil film M_f,

$$M_{fx}=\sum_{i,j}p_{i,j}r_j^2\sin\theta_i\Delta r\Delta\theta, \tag{8}$$

$$M_{fy}=\sum_{i,j}-p_{i,j}r_j^2\cos\theta_i\Delta r\Delta\theta, \tag{9}$$

the simplified overturning torque M_q:

$$\begin{cases}M_{qx}=m_sR_{cp}\sqrt{1+\tan^2\beta\cos^2\varphi}\left(\frac{\cos\beta\omega}{\cos^2\varphi+\cos^2\beta\sin^2\varphi}\right)^2 l_g\\ M_{qy}=0\end{cases} \tag{10}$$

and the friction torque M_d caused by oil-film sharing:

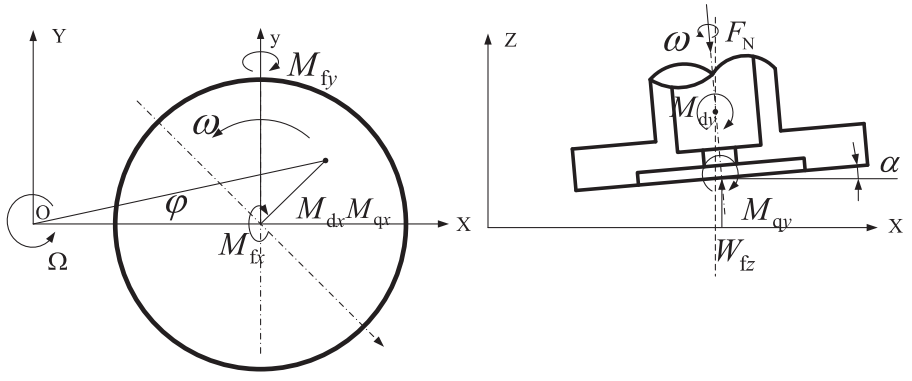

Fig. 3. Simplified mechanical model of the slipper.

$$\begin{cases} M_{dx} = 0 \\ M_{dy} = -l_h F_d \end{cases}. \tag{11}$$

The mechanical model is shown in Fig. 3.

Three balance conditions must be satisfied in the analysis: an equilibrium condition, a flow balance condition, and an extra torques balance condition. To obtain a computational model that is comparable with the experimental results, the mechanical model must be corrected. First, the tilting along the x axis caused by centrifugal load can be ignored. The tilting in the test results was attributable primarily to the shear stress in the oil. The tribo-dynamic characteristics of the slipper under the effects of spin and centrifugal loads are analyzed in the present study.

The mathematical model of the oil film shape is given as follows.

$$\begin{cases} F_N - W_{fz}(h_o, \alpha, \phi, p) = 0 \\ M_{fx}(h_o, \alpha, \phi, p_r) + M_{qx} + M_{dx} = 0 \\ M_{fy}(h_o, \alpha, \phi, p_r) + M_{qy} + M_{dy} = 0 \\ Q_{\text{out}}(h_o, \alpha, \phi, p) - Q_{\text{in}}(p) = 0 \end{cases}. \tag{12}$$

The shape of the oil film can be calculated using the equations above, but these highly nonlinear equations are difficult to solve directly. First, the Discrete Newton Algorithm is used to solve the central film thickness h_o and the pocket pressure p_s, which satisfies the balance conditions described above.

$$\text{Let } g(\alpha, \phi) = |M_{fx} + M_{qx} + M_{dx}| + |M_{fy} + M_{qy} + M_{dy}| = 0. \tag{13}$$

When the torques of the slipper are balanced, the equation above has a minimum value of zero. The solution of the film shape is simplified to an optimization problem as follows:

$$\begin{cases} \min \quad g(\alpha, \phi) = |M_{fx} + M_{qx} + M_{dx}| + |M_{fy} + M_{qy} + M_{dy}| \\ \text{s.t.} \quad 0 \leqslant \alpha \leqslant \alpha_{\max}, \quad 0 \leqslant \phi \leqslant 2\pi, \quad F_N - W_{fz} = 0, \quad Q_{\text{out}} - Q_{\text{in}} = 0, \end{cases} \tag{14}$$

where $g(\alpha,\phi)$ is the objective function and the decision variables are α and ϕ. Analytical, stochastic, and exhaustive methods are traditional methods used to solve optimization problems, but they have low efficiency and they are limited by the objective function. Thus, the NGA method is used to solve the optimization problem described above with high efficiency.

3. Solution method

3.1. NGA method

A genetic algorithm (GA) is a random search algorithm, which is loosely based on the processes of biological evolution, natural selection, and genetic mechanisms. Compared with other optimization methods, GA has a higher capacity for global optimization and it is independent of the objective function. GA is highly suitable for solving complex nonlinear problems in the field of fluid machinery [23,24]. The basic idea of the GA is to code the problem and then generate a population of a specific size. A reasonable fitness function is used to assess the performance of the gene in the population, before reproduction, crossover, and mutation are conducted as described in previous studies.

In the GA method, the 'individual' indicates a solution and the 'population' indicates a group of solutions that can be selected. 'Fitness' is the evaluation metric used to assess the performance of a gene. The 'gene' indicates the characteristic of every component of the solution.

3.2. GA parameters

(1) Decision variables:
α and ϕ. Because the tilting angle of the slipper is always very small, the constraint conditions are $0 \leqslant \alpha \leqslant 0.1°, 0 \leqslant \phi \leqslant 2\pi$. The equality constraint is as follows.

$$F_N - W = 0, \quad Q_{\text{out}} - Q_{\text{in}} = 0. \tag{15}$$

(2) Coding mode and the individual quantity of the population:
There are two genes in every chromosome. Similar to the optimization problem for hydraulic machines, the real-value encryption mode is suitable. The size of the population is 20.

(3) The individual fitness function:
The target of the problem is the minimum value of the function, thus an individual with a smaller target value corresponds to a higher fitness value. After sorting the data in order of descending target values, the fitness values of every individual is given by the following equation:

$$F_{\text{fit}} = 2\frac{P_i - 1}{N - 1}, \tag{16}$$

where F_{fit} is the fitness, P_i is the position of sorting, and N is the population size.

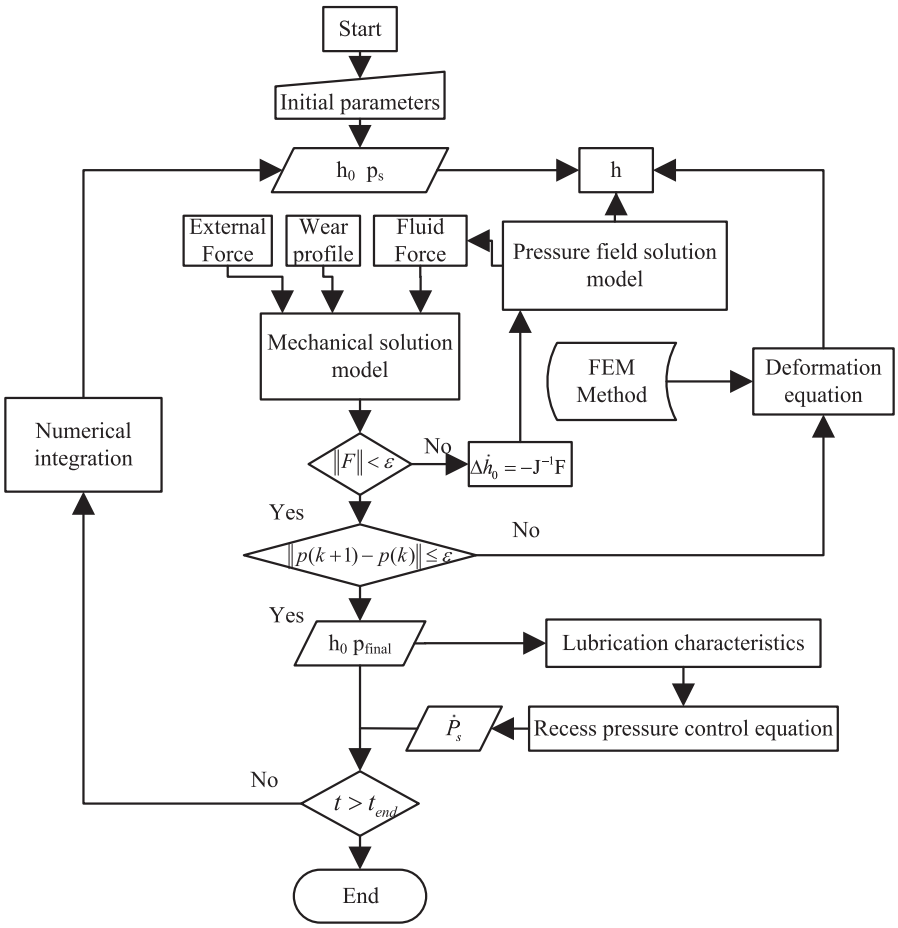

Fig. 4. Flowchart of the complete simulation.

(4) Define the GA operator:
The random ergodic sampling method is used to select the operation and the middle recombinant operator is used in the crossover operation. The nonuniform mutation operator is used in the mutation operation.
(5) The convergence conditions:
The iterations stop when the minimum value of an individual is less than 0.01.

3.3. Coupling simulation of tribo-dynamic model

Fig. 4 shows a flowchart of the complete simulation. The simulation begins with the initial parameters used as inputs, such as the working conditions, structure parameters, and initial film thickness. Next, the pressure field of the oil film is given and the film shape equation is established. The normal force governing equation is used to obtain the oil film force. The wearing profile and the deformation participate in the simulation. If the residual is sufficiently small, the lubrication characteristics are obtained. In this process, numerical integrations are used circularly. Thermal effects and roughness are not included in this coupling simulation, but it is recommended that these effects should be investigated in future studies.

4. Experimental procedures

Based on the conditions used in the simulation described above, a test bench of slipper bearings was built. The bench included a pump station, oil film testing system, driving motor, and data logging system. The test bench is shown in Fig. 5.

There are several differences between the testing system and the original pump to facilitate the acquisition of more suitable measurements.

(1) The cylinder was fixed and the swash plate could rotate.
(2) The high-low pressure transformer was canceled and oil at the same pressure was introduced into the symmetric piston chambers.

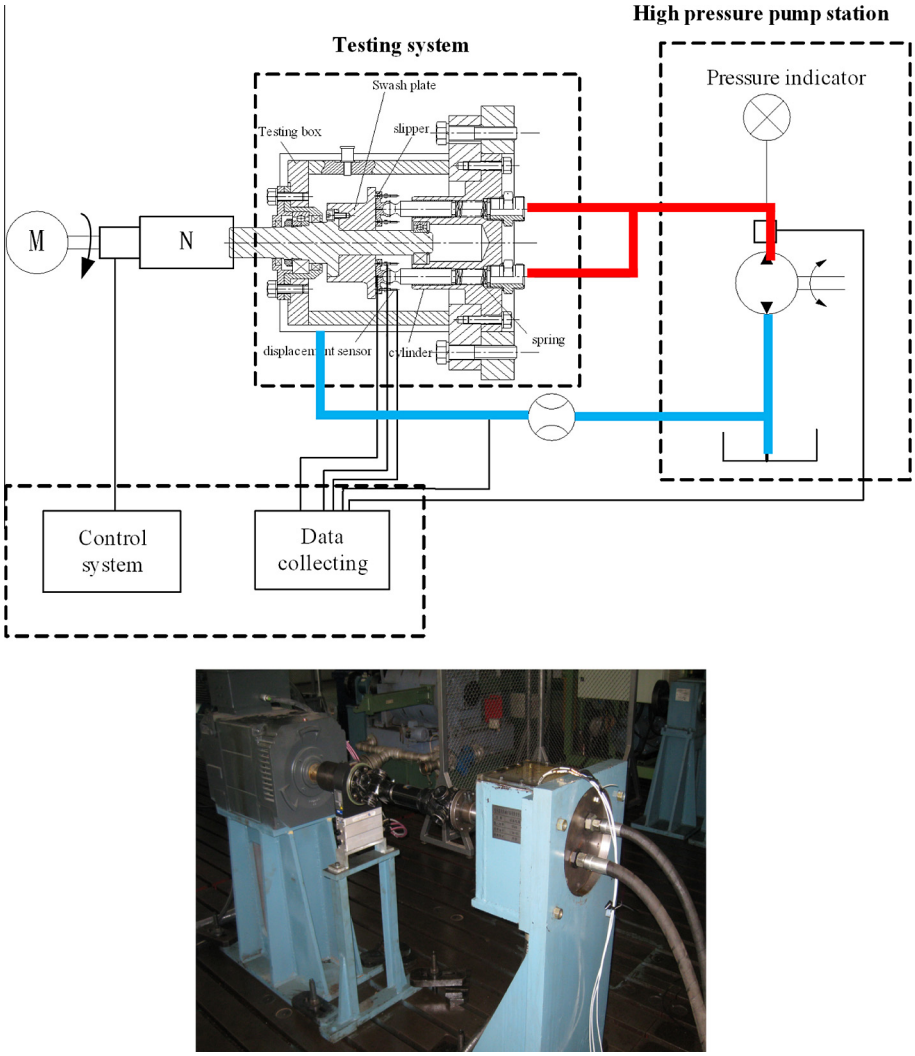

Fig. 5. Schematic (top) and photograph (below) of the test bench system.

(3) A position limiting device was installed outside the slipper to limit the spin movement.
(4) The measurement points were set outside the slipper to protect the sealing belt and the film thickness was measured indirectly.
(5) Three electric eddy displacement sensors were distributed uniformly on a ring to obtain three point oil film measurements.

The eddy sensors with wires might have been damaged by the spin of the slipper, thus a position limiting pin was used to restrain the spin motion, but without affecting the tilting. The corresponding modifications of the mathematical model were as described in Section 3. Hooke [25] showed experimentally that the tilt generated by centrifugal loads on the slipper and by the friction between the ball and its cup occurs mainly along the radial direction. This tilt does not have substantial effects on the hydrodynamic effect or the film thickness but it can change the film shape. The corresponding modification of the mathematical model was made as described in Section 3.3. In real pumps, the spin rate of the slipper increases slowly with the speed of the cylinder and the spin rate decreases at a high working pressure. For these reasons, the limitations of the slipper on a test bench under high speed and high pressure were deemed acceptable.

The oil film shape was described by a three-point method in the test and it could be transformed into the tilting description using a numerical method. The actual structure is shown in Fig. 6.

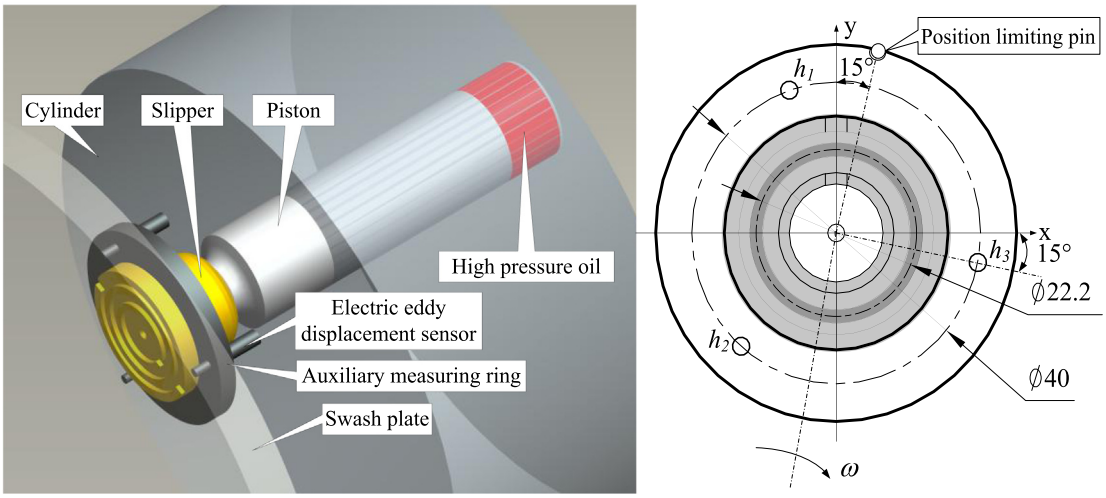

Fig. 6. Oil film thickness continuous measurement system.

5. Results and discussion

The factors that influence the slipper include the operating conditions and structural parameters. The operating conditions that can be changed included the cylinder rotating speed, oil temperature, swash plate angle, and the structure of the slipper. In the ideal state, the slipper is well lubricated and it has a long working life with low friction and low leakage. The lubrication properties have a substantial effect on performance.

The characteristics of the minimum film thickness and the central thickness are of most interest. The minimum film thickness determines the lubrication state and wearing conditions of the sealing belt, while the central film thickness reflects on the average film thickness, which is related to the anti-overturning performance. The tilting angle can be calculated from the film thickness. This angle influences the hydrodynamic effect, carrying capacity, leakage, and friction torque.

The construction data for the slipper-piston parts are given in Fig. 7.

5.1. Effects of speed on the central film thickness

Fig. 8 shows the variation in the central film thickness with rotation speed at different loading pressures with an oil dynamic viscosity of 0.025 Pa s. The red dashed lines represent the results of simulations and the black solid lines are the test results. It is noteworthy that the speed in the simulation refers to the rotational speed of cylinder, but it refers to the speed of the swash plate in the test. These two terms are equal.

With a certain swash plate angle β, the central film thickness increased with speed. This is because the hydrodynamic effects increase with high speed. Fig. 8 illustrates the trend in the decreasing central thickness with increasing working pressure. Hydrodynamic effects also strengthen with increasing working pressure. The central thickness is inversely proportional

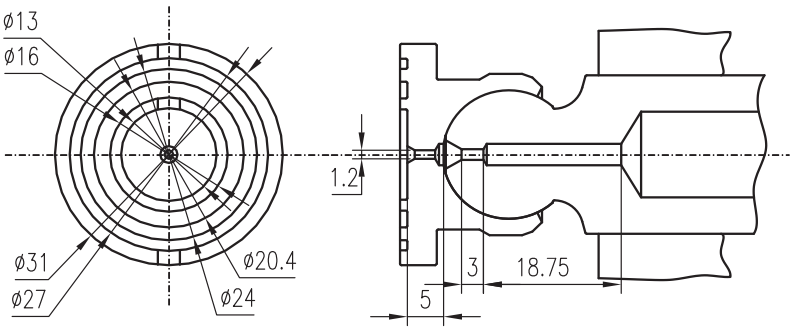

Fig. 7. Cross-section of the slipper used in the test.

to the capacity for tilting resistance. At the same time, the leakage increases with the central thickness. The film thickness determined from this model can be used to calculate parameters such as the carrying capacity, oil film torque, and leakage.

There were small differences between the simulated and experimental results. The thickness in the experiment was approximately 1 μm larger than that in the calculation. The test results also exhibited slight discontinuity, which may be due to test errors, possibly attributable to the friction of the wires and vibration in the system. These effects were observed in all of the situations evaluated.

5.2. Effects of speed on the minimum film thickness

Fig. 9 shows the variation in the minimum thickness with speed and loading pressure. The black solid lines represent the test results and the red dashed lines are the simulation results.

The general trends in the minimum film thickness were similar to those in the central thickness, which was also due to the hydrodynamic effect. Both the simulated and experimental results showed that the minimum thickness was at a very low level when the speed was low and in some conditions, h_{min} was even lower than 1 μm. In the design of a piston pump, the roughness of the swash plate and slipper bottom is up to 0.4 μm. This means that the slipper pair is in a mixed lubrication state when the working condition is at a low speed and a high pressure, which may cause severe outer cylinder wear. The frictional power loss is affected by this lubrication state. To reach the full-film lubrication state, the speed must be accelerated to a certain level to increase the hydrodynamic effect for overclamped slippers.

5.3. Effects of loading pressure on the minimum film thickness

The minimum film thicknesses with difference loading pressures are shown in Fig. 10. The black solid lines represent the test results and the red dashed lines are the simulation results. The decrease in the film thickness was approximately linearly as the pressure increased. This was because the overclamped slipper had an overclamp ratio of 1.021 when the swash plate angle was zero. This indicates that 97.94% of the oil pressure force was balanced by the maximum hydrostatic thrust force, whereas the other 2.06% of the force was carried by the hydrodynamic force. When the oil pressure increased, the unbalanced overclamp force became larger. The oil film thickness decreased to enhance the hydrodynamic effect and the carrying

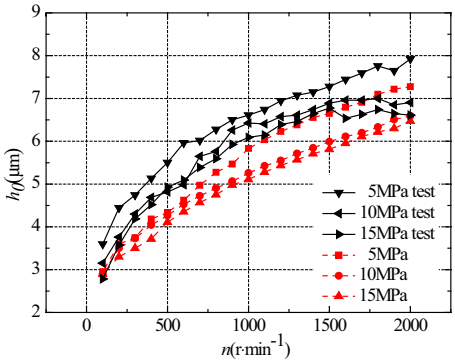

Fig. 8. Effects of speed on the central film thickness.

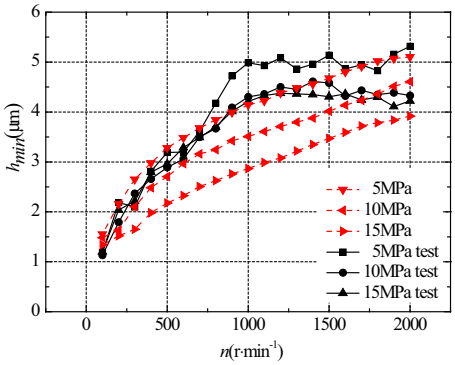

Fig. 9. Effects of speed on the minimum film thickness.

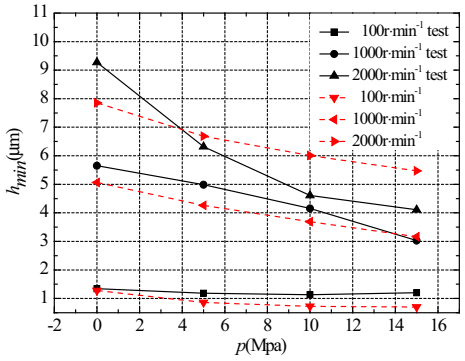

Fig. 10. Effects of pressure on the minimum film thickness.

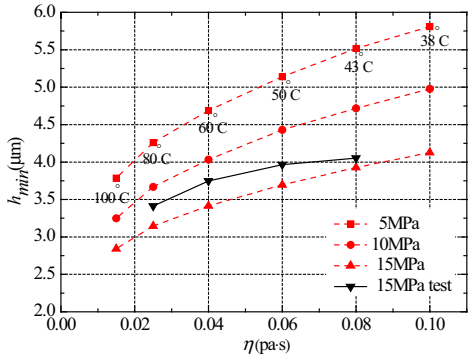

Fig. 11. Effects of oil viscosity on the minimum film thickness.

force reached a new balance. A higher speed caused a larger central thickness but less film stiffness. For these reasons, the slope of the minimum film thickness vs the pressure curve was greater at high speeds.

5.4. Viscosity of oil

Fig. 11 shows that the minimum film thickness decreased as the temperature increased in a linear manner. All of the results were obtained at a speed of 1000 rpm. The simulation results represented by red dashed lines correspond to the trend in the test results denoted by the black solid line. Thus, the simulated results agree well with the experimental values. The absolute values of the minimum thickness decreased as the supply pressure increased. The slopes of the lines were approximately equal. The viscosity influenced the hydrodynamics effects greatly; therefore, overclamped slippers are more sensitive to oil temperature than underclamped slippers.

6. Conclusions

Based on our mathematical and experimental study, the following conclusions can be made.

1. The tribo-dynamic model is a unified model that couples tribological and dynamical behaviors. The model can describe the complex behavior of both overclamped and underclamped slipper bearings. Based on the model, the effects of the operating conditions and structures on slipper bearings can be analyzed theoretically. Related problems may be addressed in the future by building on the tribo-dynamic model.
2. The NGA method is effective for the tribo-dynamic modeling of slippers because of the nonlinear characteristics of the equations. However, various solution methods can be used for different types of model. For example, the finite volume method was used in a previous study of sealing rings based on a tribo-dynamic model.
3. The hydrodynamic effect caused by rotation speed is the key factor that balances the overclamped force. The oil film forms at the same time. Both central film thickness and the minimum thickness increase with speed. The lubrication state improves as the speed increases but leakage also increases. The wearing profile and elastic deformation have substantial effects on the lubrication characteristics.

4. Both the central and minimum film thicknesses are inversely related to the loading pressure. Overclamped slippers are sensitive to the oil viscosity, thus the structural parameters should be designed well to maintain a full film state at low speed and high pressure.

Acknowledgment

This research was supported by the National Natural Science Foundation of China (Grant Nos. 51105031 and 51175039).

References

[1] M. Pelosi, M. Ivantysynova, A new fluid–structure interaction model for the slipper–swashplate interface, in: Proceedings of 5th Fluid Power Net International PhD Symposium.
[2] E. Koc, C.J. Hooke, K.Y. Li, Slipper balance in axial piston pumps and motors, J. Tribol. Trans. ASME 114 (4) (1992) 766–772.
[3] E. Koc, C.J. Hooke, Investigation into the effects of orifice size, offset and overclamp ratio on the lubrication of slipper bearings, Tribol. Int. 29 (4) (1996) 299–305.
[4] E. Koc, C.J. Hooke, Considerations in the design of partially hydrostatic slipper bearings, Tribol. Int. 30 (11) (1997) 815–823.
[5] N. Iboshi, A. Yamaguchi, Characteristics of a slipper bearing for swash plate type axial piston pumps and motors. 1. Theoretical analysis, Bull. JSME 25 (210) (1982) 1921–1930.
[6] N. Iboshi, A. Yamaguchi, Characteristics of a slipper bearing for swash plate type axial piston pumps and motors. 2. Experiment, Bull. JSME 26 (219) (1983) 1583–1589.
[7] C.J. Hooke, Y.P. Kakoullis, The effects of non-flatness on the performance of slippers in axial piston pumps, Proc. Inst. Mech. Eng. C J. Mech. Eng. Sci. 197 (DEC) (1983) 239–247.
[8] C.J. Hooke, K.Y. Li, The lubrication of overclamped slippers in axial piston pumps – centrally loaded behavior, Proc. Inst. Mech. Eng. C J. Mech. Eng. Sci. 202 (4) (1988) 287–293.
[9] M. Ivantysynova, R. Lasaar, An investigation into micro and macro geometric design of piston/cylinder assembly of swash plate machines, Int. J. Fluid Power 5 (1) (2004) 23–36.
[10] M. Ivantysynova, Ch. Huang, S.K. Christiansen, Computer aided valve plate design – an effective way to reduce noise, in: 2004 SAE International Commercial Vehicle Engineering Congress, Chicago, USA, SAE Technical Paper 2004-01-2621.
[11] F. Canbulut, E. Koc, C. Sinanoglu, Design of artificial neural networks for slipper analysis of axial piston pumps, Ind. Lubr. Tribol. 61 (2) (2009) 67–77.
[12] F. Canbulut, E. Koc, C. Sinanoglu, Experimental analysis of frictional power loss of hydrostatic slipper bearings, Ind. Lubr. Tribol. 61 (3) (2009) 123–131.
[13] N.D. Manring, C.L. Wray, Z. Dong, Experimental studies on the performance of slipper bearings within axial-piston pumps, J. Tribol. 126 (3) (2004) 511–518.
[14] S.L. Nie, G.H. Huang, Y.P. Li, Tribological study on hydrostatic slipper bearing with annular orifice damper for water hydraulic axial piston motor, Tribol. Int. 39 (11) (2006) 1342–1354.
[15] J.M. Bergada, J. Watton, J.M. Haynes, The hydrostatic/hydrodynamic behaviour of an axial piston pump slipper with multiple lands, Meccanica 45 (2010) 585–602.
[16] L. Hong, P. Zengxiong, J. Chongbo, Numerical analysis of slipper bearing's film shape in axial piston pump using genetic algorithms, J. Drainage Irrigation Mach. Eng. 1 (30) (2012) 75–79 (in Chinese).
[17] M. Kushwaha, H. Rahnejat, Z.M. Jin, Valve-train dynamics: a simplified tribo-elasto-multi-body analysis, J. Multi-body Dyn. 214 (2000) 95–110.
[18] B.K. Han, M.K. Cho, C. Kim, C.H. Lim, J.J. Kim, Prediction of vibrating forces on meshing gears for a gear rattle using a new multi-body dynamic model, Int. J. Automot. Technol. 10 (4) (2009) 469–474.
[19] Y.Y. Zhang, Y.B. Xie, D.M. Qiu, Identification of linearized oil-film coefficients in a flexible rotor-bearing system, part I: model and simulation, J. Sound Vib. 152 (3) (1992) 531–547.
[20] A. Boysal, H. Rahnejat, Torsional vibration analysis of a multi-body single cylinder internal combustion engine model, Appl. Math. Model. 21 (8) (1997) 481–493.
[21] M. De la Cruz, W.W.F. Chong, M. Teodorescu, S. Theodossiades, H. Rahnejat, Transient mixed thermo-elastohydrodynamic lubrication in multi-speed transmissions, Tribol. Int. 49 (2012) 17–29.
[22] B. Littlefair, M. De la Cruz, S. Theodossiades, Transient tribo-dynamics of thermo-elastic compliant high-performance piston skirts, Tribol. Lett. 53 (2014) 51–70.
[23] Mackle, Exeter University Savic, Walters. Application of genetic algorithms to pump scheduling for water supply, in: First International Conference on Genetic Algorithms in Engineering Systems: Innovations and Applications (GALESIA), 1995 (Conf. Publ. No. 414).
[24] X. Cai, D.C. McKinney, L.S. Lasdon, Solving nonlinear water management models using a combined genetic algorithm and linear programming approach, Adv. Water Resour. 24 (6) (2001) 667–676.
[25] C.J. Hooke, Y.P. Kakoullis, The effects of centrifugal load and ball friction on the lubrication of slippers in axial piston pumps, in: 6th Fluid Power Symposium, 1981.